Journal of Thermal Analysis, Vol. 42 (1994) 679-696

INFLUENCE OF TRANSCRYSTALLINITY ON DSC ANALYSIS OF POLYMERS
Experimental and theoretical aspects

N. Billon and J. M. Haudin

Ecole Nationale Supérieure des Mines de Paris, Centre de Mise en Forme des Matériaux, Unité de Recherche Associée au CNRS N°1374, BP 207, 06904 Sophia-Antipolis Cedex, France

Abstract

Intense parasitic nucleation has been observed at the surface of differential scanning calorimetry samples for various polymers, whereas their crystallization traces exhibit complex shapes. Revisited overall kinetics theories and computer simulation, taking into account small thickness of samples and transcrystallinity effects, allow to explain and reproduce experimental 'double peaks', currently observed with polyamide 6-6. The beginning of the transformation and the main peak are attributed to surface and bulk nucleations, respectively. As a consequence, any DSC experiment should be followed by a microscopic observation and more accurate models including thermal gradients and resistances should be developed for their interpretation.

Keywords: crystallization, DSC, polymer, transcrystallinity

1 Introduction

Crystallization of polymers, and especially crystallization during processing, is still an important field of research. Differential scanning calorimetry (DSC) is of prime importance for experimental studies. It is used either to control polymer after processing, or to determine data necessary for the prediction of their crystallization. To characterize a material in a correct way any parasitic or boundary effects must be avoided, the temperature must be well known and uniform within the sample.

Unfortunately, the circumstances of the crystallization for polymers in DSC technique are not simple and not always well controlled. The specimen is either very thin, or non-isothermal, because of the thermal conductivities which remain low in such materials. The contact between the polymer and the DSC pan may induce nucleating effects. In such a case, a big amount of additional nuclei appears close to the surface. Because of their proximity these nuclei lead to transcrystalline zones where the crystalline entities are roughly rod-shaped. The

0368–4466/94/ $ 4.00

John Wiley & Sons, Limited
Chichester

transformation induced by these nuclei competes with the 'natural' crystallization of the polymer and then, disturbs measurements.

As a consequence, DSC traces may depend, to a large extent, on non-intrinsic characteristics such as the shape of the sample or nucleating ability of DSC pans. On the other hand, classical theories often used to interpret measurements are not able to take into account such phenomena. This implies that crystallization temperatures or enthalpies, as well as data involved in models, may be erroneous. Conclusions of studies and further results of thermomechanical codes, using these values, may be inaccurate.

The purpose of this paper is to show that transcrystallinity can be often observed during DSC crystallization. Its consequences on measurements are important and can be explained and reproduced using revisited overall crystallization theories.

2 Experimental observations

2.1 Experimental procedure

When crystallization is studied, polymer is first melted between two glass slides in order to obtain films of calibrated thickness. Then, disk-shaped samples, whose diameter is equal to the diameter of DSC pans, are taken and sealed in the pans. This procedure ensures that the contact between the polymer and the pan is as good as possible, in order to minimize the effects of thermal resistances.

Samples are once again melted in the DSC apparatus, at a temperature and with a duration which ensure that they are completely molten, in order to avoid self-nucleation effects. Of course, duration and temperature depend on the polymer and are experimentally determined.

In the case of polyamides, the polymer is first dried (15 h at 80°C under vacuum), then the film is made, the sample is taken and dried again.

DSC traces are recorded and integrated to obtain curves giving $d\alpha/dt$ *vs.* time, t, where α is the transformed fraction. In the case of a constant cooling rate, this peak can be normalized by the cooling rate. Consequently, it is equivalent to the peak $d\alpha/dT$ *vs.* temperature T. For convenience we will use this representation for DSC peaks in this work.

When polymer crystallizes from the melt, semi-crystalline spherical spherulites are often formed. Spherulites consist of radial crystalline ribbons and confined amorphous polymer. They can easily be observed between crossed polarizers using thin microtomed slices and an optical microscope. Therefore, DSC samples can be observed after their crystallization. The pans are removed, thin cuts of polymer are taken and observed with a microscope.

2.2 *Transcrystallinity during DSC experiments*

2.2.1 Introduction

In the case of various polymers, such as polybutene-1 (Fig. 1a) or polyamide 6-6 (Fig. 1b), one can often observe a lot of nuclei on the surfaces which were in contact with the pans. Due to their proximity, these nuclei lead to one-dimensional morphologies which grow perpendicular to the surfaces. They form two transcrystalline zones.

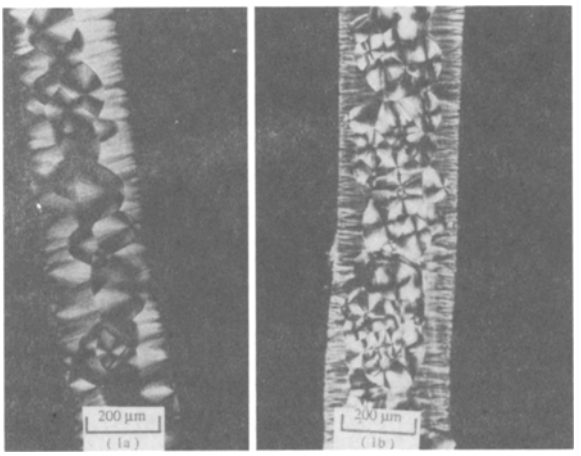

Fig. 1 Typical microtomed cross-sections of DSC specimens in the case of a polybutene-1 (a), and a polyamide 6-6 (b) in presence of transcrystallinity

The nucleating ability of aluminium, or more likely of alumina (Al_2O_3), has already been demonstrated for various polymers [1, 2]. Such an effect has also been reported in DSC analysis of high density polyethylene [3, 4] and polypropylene [5].

In these cases DSC samples contain two kinds of nuclei:

* Those which are distributed in the volume, or volume nuclei.
* Those which are located close to the surfaces, or transcrystalline nuclei.

Transformation results from the competition between these two nucleation processes. Transcrystalline nuclei must be regarded as parasitic nuclei, inducing a disturbing effect.

2.2.2 DSC traces

Concurrently to these optical observations, DSC traces may have complex shapes. For instance, in the case of polyamide 6-6 (Fig. 2), shoulder-shaped or

double peaks [6, 7] are often observed when transcrystallinity occurs. Similar observations have been reported in the literature concerning polymers which crystallize in contact with a nucleating surface (fibers or bulk materials), either during isothermal [8, 9] or anisothermal experiments [9, 10].

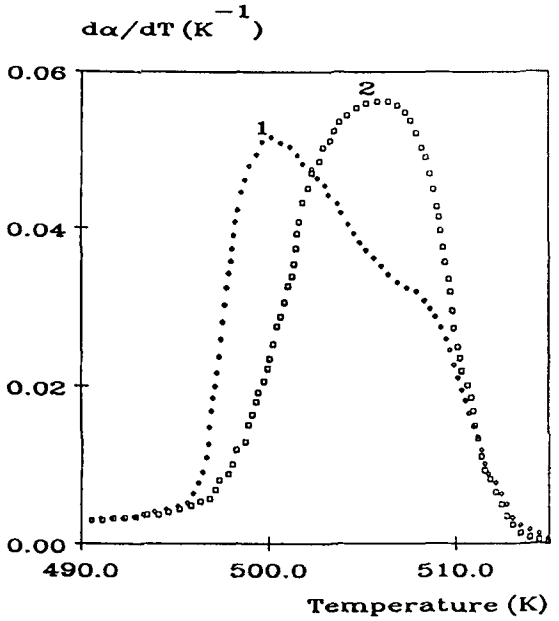

Fig. 2 Experimental DSC peaks at a 10 deg·min^{-1} cooling rate. Comparison between a given polymer (1) and the same polymer with a nucleating agent (2) [11]

The shape of DSC traces may also vary with the number of nuclei existing in the polymer. These effects can be illustrated by experiments performed on an injection-molding PA 6-6 grade in which transcrystalline effects are known to be important [11]. When a nucleating agent, promoting volume nucleation, is added to the polymer, the shoulder-shaped peak becomes a single one, and its maximum is shifted towards higher temperature (Fig. 2). The same kind of observations has been done on polyethylene [4]: the less numerous the volume spherulites, the lower the crystallization temperature (as defined by the temperature of the maximum of the crystallization peak).

On the other hand, in the case of polyethylene [4], as well as in the case of polyamide 6-6 [7], the more numerous the volume nuclei, the less important the transcrystalline zones. It can be concluded, as already suggested by other authors [4, 5], that bulk nucleation, competing with surface nucleation, determines the final thickness of the transcrystalline zones.

2.3 Thickness effects during DSC experiments

Generally, polymers have a low thermal conductivity. So, thermal gradients may occur within DSC samples. In such a case two solutions can be adopted:

* First, to solve energy equation using anisothermal crystallization models [12, 13] in order to develop models for the DSC calorimeter, also including thermal resistances [14].

* Second, to use thin samples (i.e., 300 μm or less) to ensure negligible thermal gradients.

Nevertheless, since STEIN and POWERS [15], it is known that the transformation is different in a thin film and in an infinite volume. Different theoretical approaches make it possible to calculate the average transformed volume fraction in a thin film during isothermal [16, 17] or anisothermal [17, 18] transformations. They clearly show that the transformation is slower in a thin film. As a consequence, experimental results may depend on the thickness of the sample.

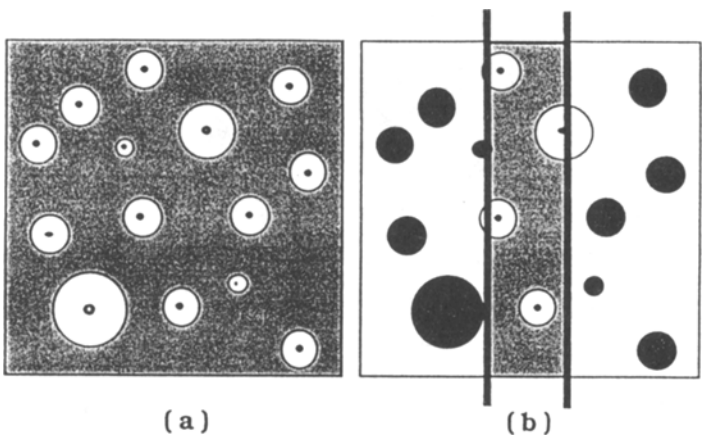

Fig. 3 Schematic explanation for volume limitation effects. Comparison between an infinite (a) and a limited volume (b)

A simple explanation for this phenomenon can be given. Let us consider an infinite volume (Fig. 3a), the average transformed volume fraction is in fact the probability for any point of the volume to be transformed at the considered time. This probability is related to the number of activated spherulites which surround the point and which are able to have reached it since the beginning of the crystallization. If the volume is reduced to a film (Fig. 3b) the probability for each point of the film to be transformed decreases, since some spherulites will disappear (e.g., the black ones in Fig. 3b). Consequently, the rate of transformation of the whole film decreases.

Obviously, the crystallization is sensitive to that effect when one of the dimensions of the sample (i.e., its thickness) is of the same order of magnitude as the mean radius of spherulites. This occurs sometimes, i.e., in the case of polybutene-1 (Fig. 4).

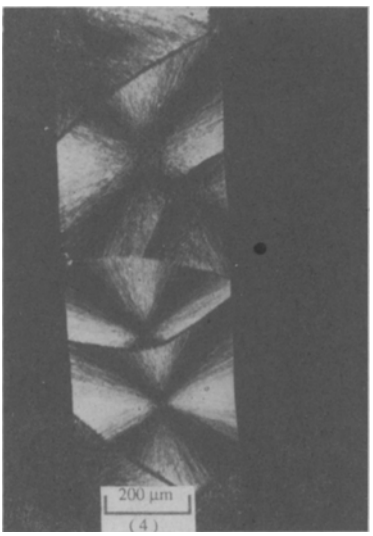

Fig. 4 Microtomed cross-section of a DSC specimen of polybutene-1 (cooling rate 10 deg·min^{-1})

In addition, it must be noticed that the relative importance of transcrystallinity increases as the thickness decreases, so that transcrystallinity and small thickness must be taken into account simultaneously.

2.4 Conclusion

From above observations it can be concluded that to interpret DSC measurements in a good way one must, at least, take into account:

* The thickness of the sample.
* Transcrystallinity effects.

These two parasitic effects have been encountered with various polymers and reported in the literature.

Abnormal results, such as shouldered peak, have been observed concurrently with transcrystallinity, either in our own experiments, or in the literature. It would be interesting to establish the relationship between peak shapes and transcrystallinity.

3. Modelling of transcrystallinity effects

3.1 Introduction

Two different means have been used:

* First, a computer simulation of the crystallization.
* Second, a theoretical approach developed within the frame of the overall crystallization kinetics theories.

Both these two approaches are based on the same general description for the crystallization of polymers.

3.2 General description for crystallization of polymers

Classical models for overall kinetics theories [19–23] are statistical approaches, and are equivalent [26]. Within the frame of these models, crystallization is decomposed into the appearance, or nucleation, and the growth of spherical (or disk-, or rod-shaped) semi-crystalline entities (spherulites). Spherulites overlap the whole volume of the specimen without overlapping one another. At any time t, the transformation is characterized by the transformed volume fraction, α, which is the fraction of volume overlapped by spherulites. It is expressed as a function of nucleation and growth parameters.

Nucleation parameters are:

* A nuclei density, N_o, or number of potential nuclei per unit volume. These are points of the material where nucleation can occur. They are assumed to pre-exist in the polymer and they become growing entities through an activation process.
* A probability per unit of time of such an activation or activation frequency, q.

As soon as a nucleus is activated it grows, at a growth rate G, till it impinges on another spherulite. G and q do not depend upon time, conversely they depend on temperature. N_o, for its part, depends on the thermal treatment preceeding the crystallization but neither on time, nor on crystallization temperature.

3.3 Computer simulation

Computer simulation is based on the general description for crystallization and is an anisothermal extension of a previous isothermal simulation [24]. The sample, assumed to be a parallelepiped, contains potential nuclei randomly distributed with an initial number per unit volume N_o. Nuclei are activated at ran-

dom with an average activation frequency q. Both activation time and location of the nuclei are determined using the random number generator of our computer. A potential nucleus which has been overlapped by a previously activated entity cannot be activated. On the contrary, if it is located in a still liquid region, it can be activated and immediately gives rise to a sphere whose growth rate is G. To model transcrystallinity, additional nuclei are added on two parallel surfaces of the parallelepiped. Transcrystalline nuclei have different 'nucleation characteristics' N_S and q_s.

The program calculates:

* The radii of the spherulites.
* Their actual shapes, taking into account the boundaries between them.

Then, the code can draw planar sections of the simulated morphologies (in the present case, parallel and perpendicular to the 'transcrystalline' surfaces).

3.4 Theoretical approach

In the initial version of overall crystallization kinetics theories:

* The volume of the sample is assumed to be infinite.
* The temperature is assumed to be homogeneous within the sample.
* The sample is assumed to contain only one kind of nuclei.
* These nuclei are assumed to be homogeneously distributed within the sample.

As a consequence, and taking into account the above experimental observations (Section 2), these assumptions have to be avoided to model DSC experiments.

Our approach is based on a rigorous analysis of the classical theory [25, 26] which leads to a more general expression for α. Our new model allows us to consider cases where:

* There are several kinds of nuclei in the polymer, each of them being characterized by a density and an activation frequency.
* All nuclei lead to the same kind of growing entities, that is, having the same growth rate, G, and the same geometry.
* Any kind of nuclei can be non-homogeneously distributed, that is, in particular located in zones close to the surfaces, or homogeneously distributed within the volume. To achieve this point, N_0 is taken as a function of spatial coordinates.
* The isokinetic assumption [20] (G/q constant) is valid for any kind of nuclei.

* Any cooling conditions can be modelled but temperature must be homogeneous in the polymer, (i.e., at least at the scale of crystallization phenomena).

When applied to the case of a thin film having infinite width and length and a finite thickness this model seems to be more accurate for DSC measurements than initial theories.

Complete calculations have been presented elsewhere [7, 18, 25, 26] and would be beyond the scope of the present paper. Let us present the main results. Transformed fraction varies within the thickness of the film and can be written locally at each point of the film as a function of its abscissa, X_a. Obviously, it also depends on time t, or more precisely on the maximum radius for

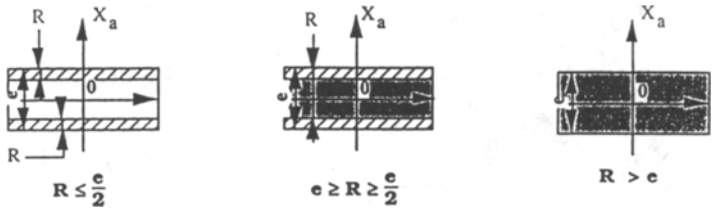

$$\alpha = \frac{2}{e}\int_0^{e/2}\left[1 - \exp\left(-E(X_a, t)\right)\right] dX_a$$

R	$\lvert X_a \rvert$		$E(X_a, t)$
$R \le \frac{e}{2}$	$\lvert X_a \rvert < \left(\frac{e}{2} - R\right)$		$8\pi\left[\frac{G}{q}\right]^3 N_0\, f(\eta_t)$
$R \le \frac{e}{2}$	$\lvert X_a \rvert \ge \left(\frac{e}{2} - R\right)$		$8\pi\left[\frac{G}{q}\right]^3 N_0 \left[f(\eta_t) + \left(\frac{\gamma_1}{4} - \frac{1}{2}\right) f(\eta_{x1}) - \frac{\gamma_1}{24}\eta_{x1}^3\right]$ + $2\pi\left[\frac{G}{q_S}\right]^2 N_S \left[(\phi_1 - 1)\, g(\kappa_{x1}) + \frac{1}{2}\phi_1 \kappa_{x1}^2\right]$
$R > \frac{e}{2}$	$\lvert X_a \rvert < \left(R - \frac{e}{2}\right)$		$8\pi\left[\frac{G}{q}\right]^3 N_0 \left[f(\eta_t) + \left(\frac{\gamma_1}{4} - \frac{1}{2}\right) f(\eta_{x1}) - \frac{\gamma_1}{24}\eta_{x1}^3 + \left(\frac{\gamma_2}{4} - \frac{1}{2}\right) f(\eta_{x2}) - \frac{\gamma_2}{24}\eta_{x2}^3\right]$ + $2\pi\left\{\frac{G}{q_S}\right\}^2 N_S \left\{(\phi_1 - 1)\, g(\kappa_{x1}) + \frac{1}{2}\phi_1 \kappa_{x1}^2 + (\phi_2 - 1)\, g(\kappa_{x2}) + \frac{1}{2}\phi_2 \kappa_{x2}^2\right\}$

Fig. 5 Expressions for α in the case of a thin film in presence of transcrystallinity. Parameters are defined in Table 1

spherulites, R (Table 1). Average transformed fraction of the film, α, is calculated through integration. Results are presented in Fig. 5 and Table 1.

Table 1 Definiton of parameters used in Fig. 5

Volume spherulites	Transcrystalline spherulites
$\gamma_1 = \frac{q}{G}\left(\frac{e}{2} - \lvert X_a \rvert\right)$	$\varphi_1 = \frac{q_s}{G}\left(\frac{e}{2} - \lvert X_a \rvert\right)$
$\gamma_2 = \frac{q}{G}\left(\frac{e}{2} + \lvert X_a \rvert\right)$	$\varphi_2 = \frac{q_s}{G}\left(\frac{e}{2} + \lvert X_a \rvert\right)$
$\eta_{x1} = \eta_t - \gamma_1$	$\kappa_{x1} = \kappa_t - \varphi_1$
$\eta_{x2} = \eta_t - \gamma_2$	$\kappa_{x2} = \kappa_t - \varphi_2$
$\eta_t = \int_0^t q(u)\,du$	$\kappa_t = \int_0^t q_s(u)\,du$
$f(\eta) = \exp(-\eta) - 1 + \eta - \frac{\eta^2}{2} + \frac{\eta^3}{6}$	$g(\kappa) = \exp(-\kappa) - 1 + \kappa - \frac{\kappa^2}{2}$
$R = \int_0^t G(u)\,du$	

3.5 Conclusion

Simulation allows us to reproduce both the DSC measurement and the microtomed sections, whereas calculation allows to reproduce only the evolution of the transformed volume fraction. These two approaches are in very good agreement in any case we tested.

4. Results and discussion

4.1 Preliminary remarks

Let us now consider a polymer, which could be a polyamide 6-6, and its growth rate G [27]:

$$G = 9.87 \cdot 10^4 \exp\left(\frac{-6270}{8.32\,(T(\mathrm{K}) - 303)}\right) \exp\left(\frac{-1.89 \cdot 10^5}{T(\mathrm{K})\,(553 - T(\mathrm{K}))}\right) \mu\mathrm{m/s} \quad (1)$$

Using simulation and analytical calculations it is possible to consider three typical cases (Fig. 6):

* A case where there are no volume nuclei ($N_o = 0$).
* A case where there are a few nuclei ($N_o = 5 \cdot 10^{-6}$ μm^{-3}).
* A case where there are a lot of nuclei ($N_o = 3 \cdot 10^{-5}$ μm^{-3}).

Microtomed slices (Fig. 6a) and DSC peaks (Fig. 6b) can be reproduced.

In the intermediate case the main peak is preceeded by a shoulder which disappears in the third one. This is in good agreement with experimental effects of a nucleating agent (Fig. 2): increasing the number of spherulites displaces the main peak towards higher temperature and makes the shoulder disappear. In the same way the thickness of transcrystalline zones decreases when N_o increases (Section 2) as related in the literature [4, 5].

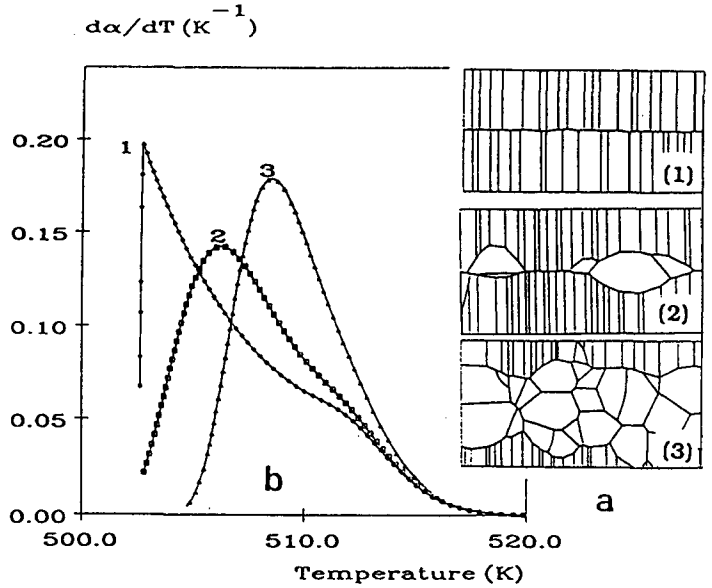

Fig. 6 Simulated effects of transcrystallinity on microtomed sections (a) and $d\alpha/dT$ peaks (b) for a 100 μm-thick film in three cases of volume nucleation: (1) $N_o = 0$ μm^{-3}; (2) $N_o = 5 \cdot 10^{-6}$ μm^{-3}; (3) $N_o = 3 \cdot 10^{-5}$ μm^{-3} (Growth rate is given by Equation (1), cooling rate is 10 deg·min^{-1}, $N_S = 10^{-2}$ μm^{-2}, $G/q_s = 10^{-5}$ μm, $G/q = 1$ μm)

At this stage, it can be concluded that the shapes of the DSC peaks, $d\alpha/dT$ *vs.* temperature, are well related to transcrystallinity and that we can reproduce aspects of both microtomed sections and DSC traces.

4.2 Shapes of the peaks: physical explanations

If we now focus on the first case ($N_o = 0$) in Fig. 6, that is, without any volume nucleation, we can see that the shoulder remains present. This suggests

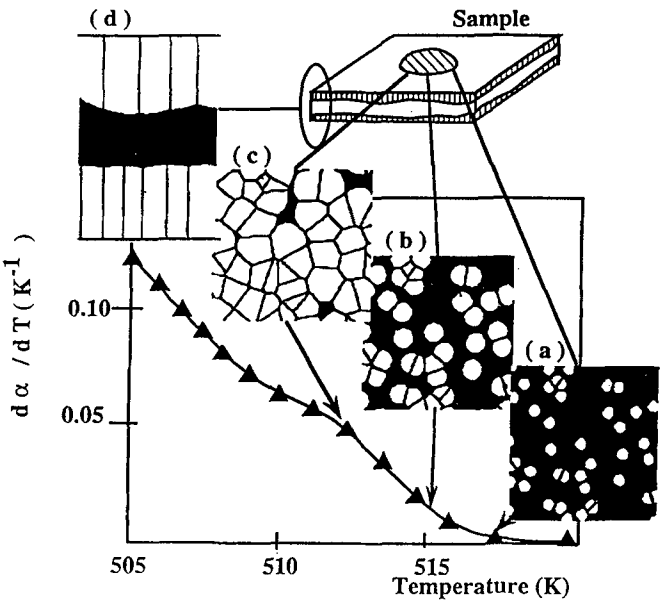

Fig. 7 Formation of the shoulder-shaped peaks observed on DSC traces in presence of transcrystallinity. Evolution of the morphology of the 'sample' and of the calculated $d\alpha/dT$ in the same case as Fig. 6 (1)

that the beginning of all peaks, especially the shoulder, is governed by transcrystallinity. This can be demonstrated using computer simulation to simulate planar sections parallel (Figs 7a, 7b and 7c) and perpendicular (Fig. 7d) to the 'transcrystalline' surfaces at different steps of the transformation.

At the very first steps of the transformation, the transformed volume consists of distinct semi-spherical spherulites (Figs 7a and 7b). Let N_S, S and e be the density of spherulites existing on the surfaces, the area of each surface and the thickness of the film, respectively. Transformation kinetics is well approximated by (Fig. 8):

$$\begin{cases} \alpha = \dfrac{4\pi}{3}\cdot\dfrac{N_S}{e}\left[\displaystyle\int_o^t G(u)\mathrm{d}u\right]^3 \\ \dfrac{\partial\alpha}{\partial t} = 4\pi\,\dfrac{N_S}{e}\,G(t)\left[\displaystyle\int_o^t G(u)\mathrm{d}u\right]^2 \end{cases} \tag{2}$$

where $G(u)$ is the growth rate at time u ranging from 0 to time t.

As the spherulites grow, their growth is progressively limited to directions more or less perpendicular to the surfaces. Step by step, the transformed volume becomes more 'compact' (Fig. 7c) and the transformation finally results in the growth of two continuous planar fronts coming from the surfaces (Fig. 7d). Then (Fig. 8):

$$\begin{cases} \alpha = \dfrac{2}{e}\left[\displaystyle\int_0^t G(u)\,du\right] \\ \dfrac{\partial\alpha}{\partial t} = \dfrac{2}{e}\,G(t) \end{cases} \tag{3}$$

So, the transformation rate $\partial\alpha/\partial t$, or $\partial\alpha/\partial T$, progressively changes from a form described by Eq. (2) to an expression where it becomes proportional to G (Eq. (3)). This change, which is well modelled by our calculations (Fig. 8), corresponds to a slowing down of the kinetics. It is responsible for the shoulder observed in the DSC traces (Section 2).

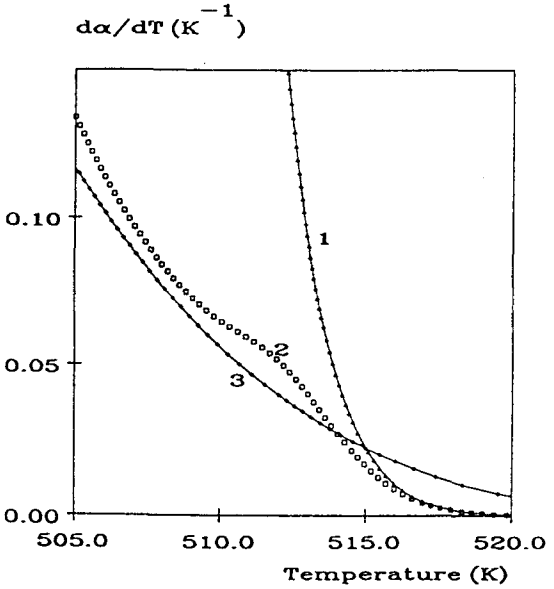

Fig. 8 Comparison between our model (2), the cases of independent half-spheres (1) (Eq. (2)) and continuous planar fronts (3) (Eq. (3)), in the same case as Fig. 6 (1)

This analysis confirms that the shoulder at the beginning of DSC peak can be unambiguously related to the transcrystalline zones. Furthermore, it is due

to a change in the transformation kinetics, from half-spheres to continuous fronts.

4.3 Effects of thermal gradients

To minimize the influence of transcrystallinity, one might choose to increase the thickness of the samples. Unfortunately, due to thermal conductivity of polymers, this may induce thermal gradients and also lead to inaccurate measurements. To try to estimate the order of magnitude of perturbations it is necessary to solve energy equation taking into account crystallization kinetics, i.e., to solve energy equation written in terms of the enthalpy per unit mass [12, 13]. In addition, a kinetic law must be chosen, e.g. for convenience, a simplified form [12, 13] based on measurements performed during crystallization at constant cooling rates, $\dot{T}$. In the latter case [28]:

$$\alpha(t) = 1 - \exp\left[-\frac{\chi(T(t))}{|\dot{T}|^n}\right] \tag{4}$$

where $\chi(T(t))$ is an experimental parameter [28] which depends only on the temperature.

It is possible to calculate the evolutions of temperature and transformed fraction during time. Recalculated peak $d\alpha/dt$ can then be compared to the expected results.

Table 2 Data used in calculation of Fig. 9

Parameter	Value	Unit
$\dot{T}$	0.333	$K \cdot s^{-1}$
χ	$-0.7103814T(K)+348.695$	$[K \cdot s^{-1}]^n$
n	3	-
Enthalpy of crystallization	$5.434 \cdot 10^4$	$J \cdot kg^{-1}$
Thermal conductivity	0.23	$W \cdot m^{-1} \cdot K^{-1}$
Specific heat	1 672	$J \cdot kg^{-1} K^{-1}$
Density	980	$kg \cdot m^{-3}$

In the case of parameters which are representative of a polyamide 6-6, (Table 2) and for a 600 μm-thick film cooled at its surfaces at a constant cooling rate of 20 $deg \cdot min^{-1}$, thermal gradient between the core and the surfaces does not exceed 0.5 degree. Despite the weakness of this value, the peak is broader and the maximum is displaced towards higher times (Fig. 9). In conclusion,

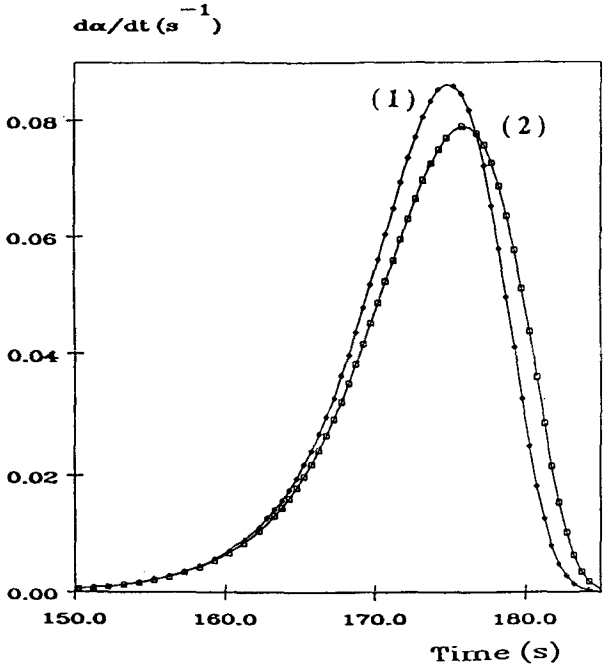

Fig. 9 Comparison between expected (1) and actual DSC peak (2) as calculated using an-isothermal model and data given in Table 2

gradient effects must not be neglected in DSC analysis. Even a 600 μm-thick film may be regarded as a thick film.

5. Conclusions

Transcrystallinity may occur during DSC experiments. It has been observed on very different kinds of polymers. Due to the small size of the sample the effects of this parasitic phenomenon may be very important. Experimental observation enables us to relate the shoulder-shaped form of some DSC traces to transcrystallinity. Furthermore, the shape of the peak and the temperature at the maximum depend to a large extent on the efficiency of nucleation within the polymer.

Revisited overall crystallization kinetics theory makes it possible to explain and reproduce experimental observations. Computer simulation enables us to reproduce the aspect of microtomed sections.

In presence of transcrystallization the DSC peak may adopt a shoulder shaped form which can be decomposed as follows:

* At the very beginning, the transformed fraction is proportional to the third power of the maximum radius for spherulites, since transformation is mainly due to distinct half-spherulites originating from the surfaces of the DSC sample.

* Progressively, it becomes proportional to this maximum radius, as these spherulites impinge on one another and form a more or less planar continuous front.

* Between these two phases, a shoulder appears, which is due to this change in transformation kinetics.

* Volume nucleation is responsible for both the location of the maximum of the peak and the final thickness of transcrystalline zones.

Generally, actual shapes of peaks are governed by a competition between volume and transcrystalline nucleation. As a consequence, they may have various and different forms depending on nucleating agent, thickness of the samples, cooling rate.

The effects of transcrystallization are now well recognized and further work would consist in developing a complete model for DSC measurements. It must be noticed, here, that this complete model should take into account actual nucleation, of course, but also thermal gradients and thermal resistances between furnaces and samples [14]. Meanwhile, it must be emphasized that it is necessary to observe microtomed slices of DSC samples before any conclusion in order to ensure that neither transcrystallinity, nor volume limitation occur during measurements.

List of the symbols

E	Mathematical expectancy
e	Thickness of the sample
$f_{(\eta)}$	Mathematical function related to volume nucleation (Table 1). η is equal to, either η_t, η_{x1} or η_{x2}.
G	Growth rate of the spherulites
$g(\kappa)$	Mathematical function related to surface nucleation (Table 1). κ is equal to, either κ_t, κ_{x1} or κ_{x2}
N_o	Initial density of potential nuclei in the volume
N_S	Initial density of potential nuclei at the surface
n	Avrami exponent
q	Activation frequency for the potential nuclei in the volume

q_s	Activation frequency for the potential nuclei at the surface
R	Maximum radius for a spherulite
T	Temperature
$\dot{T}$	Cooling rate
t, u	Time
X_a	Abscissa of any point of the sample (ranging from $-e/2$ to $+e/2$
α	Transformed volume fraction
χ	Ozawa parameter
γ_1, γ_2, η_t, η_{x1}, η_{x2}	Adimensional parameters related to volume nuclei (Table 1)
φ_1, φ_2, κ_t, κ_{x1}, κ_{x2}	Adimensional parameters related to surface nuclei (Table 1)

References

1 A. M. Chatterjee and F. P. Price, J. Polym. Sci., Polym. Phys. Ed., 13 (1975) 2369.
2 A. M. Chatterjee and F. P. Price, J. Polym. Sci., Polym. Phys. Ed., 13 (1975) 2391.
3 M. R. Kamal and E. Chu, Polym. Eng. Sci, 23 (1983) 27.
4 G. V. Fraser, A. Keller and J. A. Odell, J. Appl. Polym. Sci., 22 (1978) 2979.
5 H. Janeschitz-Kriegl, Progr. Colloid Polym. Sci., 87 (1992) 117.
6 N. Billon, C. Magnet and J. M. Haudin, Eighth Annual Meeting of the Polymer Processing Society, New Dehli, 1992.
7 N. Billon, C. Magnet, J. M. Haudin and D. Lefebvre, Colloid Polym. Sci., (1994), to be published.
8 M. R. Kantz and R. D. Corneliussen, J. Polym. Sci., Polym.Lett. Ed., 11 (1973) 279.
9 T. He and R. S. Porter, J. Appl. Polym. Sci., 35 (1988) 1945.
10 M. G. Huson and W. J. Mc Gill, J. Polym. Sci., Polym. Chem. Ed., 22 (1984) 3571.
11 F. D. Pretel, Internal Report, Mastère MATMEF, Ecole Nationale Supérieure des Mines de Paris 1991.
12 J. M. Haudin and N. Billon, Progr. Colloid Polym. Sci., 87 (1992) 132.
13 N. Billon, Ph. Barq and J. M. Haudin, Int. Polym. Proc., 6 (1991) 348.
14 C. H. Wu, G. Eder and H. Janeschitz-Kriegl, Colloid Polym. Sci., 271(1993) 1116.
15 R. S. Stein and J. Powers, J. Polym. Sci., 56 (1962) S9.
16 J. M. Escleine, B. Monasse, E. Wey and J. M. Haudin, Colloid Polym. Sci., 262 (1984) 306.
17 N. Billon, J. M. Escleine and J. M. Haudin, Colloid Polym. Sci., 267 (1989) 668.
18 N. Billon and J. M. Haudin, Colloid Polym. Sci., 267 (1989) 1064.
19 A. N. Kolmogoroff, Izvest. Akad. Nauk. SSR, Ser. Math., 1 (1937) 335.
20 M. Avrami, J. Chem. Phys., 7 (1939) 1103.

21 M. Avrami, J. Chem. Phys., 8 (1940) 212.
22 M. Avrami, J. Chem. Phys., 9 (1941) 177.
23 U. R. Evans, Trans. Faraday Soc., 41 (1945) 365.
24 N. Billon and J. M. Haudin, Ann. Chim. Fr., 15 (1990) 1.
25 N. Billon, Thesis, Ecole Nationale Supérieure des Mines de Paris, 1987.
26 N. Billon and J. M. Haudin, Ann. Chim. Fr., 15 (1990) 173.
27 C. Magnet, Internal Report, Ecole Nationale Supérieure des Mines de Paris, CEMEF, 1990.
28 T. Ozawa, Polymer, 12 (1971) 150.

Zusammenfassung — Bei verschiedenen Polymeren wurde an der Oberfläche von DSC-Proben eine intensive parasitäre Keimbildung beobachtet, während ihre Kristallisation komplexe Formen zeigt. Überarbeitete gesamtkinetische Theorien und Computersimulation unter Berücksichtigung dünner Probenstärken und Transkristallinitätseffekte ermöglichen die Deutung und die Reproduzierung experimenteller "Doppelpeaks", wie sie wie in diesem Falle bei Polyamid 6-6 beobachtet werden. Der Beginn der Umwandlung beziehungsweise der Hauptpeak werden der Keimbildung an der Oberfläche beziehungsweise im Inneren zugeschrieben. Als Folge davon sollten alle DSC-Experimente von einer mikroskopischen Untersuchung gefolgt werden und für deren Interpretation sollten präzisere Modelle unter Einbezug von thermischem Gradient und Widerstand entwickelt werden.